

Turbulent dynamo in a collisionless plasma

François Rincon^{*†}, Francesco Califano[‡], Alexander A. Schekochihin^{§¶} and Francesco Valentini^{||}

^{*}Université de Toulouse; UPS-OMP; IRAP; Toulouse, France, [†]CNRS; IRAP; 14, avenue Edouard Belin, F-31400 Toulouse, France, [‡]Physics Department, University of Pisa, 56127 Pisa, Italy, [§]The Rudolf Peierls Centre for Theoretical Physics, University of Oxford, 1 Keble Road, Oxford, OX1 3NP, United Kingdom, [¶]Merton College, Oxford OX1 4JD, United Kingdom, and ^{||}Dipartimento di Fisica, Università della Calabria, I-87036 Rende (CS), Italy

Submitted to Proceedings of the National Academy of Sciences of the United States of America

Magnetic fields pervade the entire Universe and affect the formation and evolution of astrophysical systems from cosmological to planetary scales. The generation and dynamical amplification of extragalactic magnetic fields through cosmic times, up to μ Gauss levels reported in nearby galaxy clusters, near equipartition with kinetic energy of plasma motions and on scales of at least tens of kiloparsecs, is a major puzzle largely unconstrained by observations. A dynamo effect converting kinetic flow energy into magnetic energy is often invoked in that context, however extragalactic plasmas are weakly collisional (as opposed to magnetohydrodynamic fluids), and whether magnetic-field growth and sustainment through an efficient turbulent dynamo instability is possible in such plasmas is not established. Fully kinetic numerical simulations of the Vlasov equation in a six-dimensional phase space necessary to answer this question have until recently remained beyond computational capabilities. Here, we show by means of such simulations that magnetic-field amplification via a dynamo instability does occur in a stochastically-driven, non-relativistic subsonic flow of initially unmagnetized collisionless plasma. We also find that the dynamo self-accelerates and becomes entangled with kinetic instabilities as magnetization increases. The results suggest that such a plasma dynamo may be realizable in laboratory experiments, support the idea that intracluster medium (ICM) turbulence may have significantly contributed to the amplification of cluster magnetic fields up to near-equipartition levels on a timescale shorter than the Hubble time, and emphasize the crucial role of multiscale kinetic physics in high-energy astrophysical plasmas.

magnetic fields | dynamo | turbulence | intracluster medium

The generation, amplification and sustainment of magnetic fields in Nature may be driven by a variety of physical processes, an important family of which are dynamo instabilities converting kinetic energy of chaotic flows into magnetic energy. While fluid (collisional) magnetohydrodynamic (MHD) dynamos relevant to the planetary, stellar and galactic contexts had long been thought possible on the basis of idealized theoretical models of turbulent flows [1, 2, 3, 4], a major boost to their understanding was given by early pioneering numerical simulations of magnetic field amplification by 3D MHD turbulence [5], a rare case of proof-of-principle “numerical discovery” later followed by experimental evidence using liquid metals [6]. Dynamos in weakly-collisional plasmas, in spite of their potential relevance to cosmic magnetogenesis [7, 8] on extragalactic scales [9, 10, 11, 12, 13, 14, 15, 16, 17, 18], have thus far not achieved such a milestone. Although dedicated laboratory experiments are under development [19, 20], the interactions between dynamos, collisionless damping and kinetic-scale phenomena related to plasma magnetization are poorly understood. Magnetization occurs when the field has grown sufficiently that the particles’ Larmor radius becomes smaller than the typical size ℓ of velocity fluctuations. It does not take much field to achieve this: in the ICM, taking $\ell = 1$ kiloparsec and $\sim 10^7$ K ion temperature, ions are magnetized for fields above 10^{-13} Gauss, well below the level at which magnetic energy reaches equipartition with kinetic energy of plasma motions. Past this stage, any local change in magnetic-field strength due to compressive or shearing motions will generate pressure anisotropies with respect to the field by virtue of magnetic-moment conservation, rendering the plasma everywhere unstable to fast kinetic instabilities [12], with potentially critical implications for magnetic growth and dynamics [16, 17, 21, 22, 23, 24, 25, 26, 27]. Demonstrating whether colli-

sionless plasma dynamos exist and how they work requires solving Vlasov-Maxwell equations in three physical space dimensions (3D, this stems from antidynamo theorems in 2D [4]), plus three velocity space dimensions (3V). We performed the first numerical simulations of this problem, which show that magnetic-field amplification

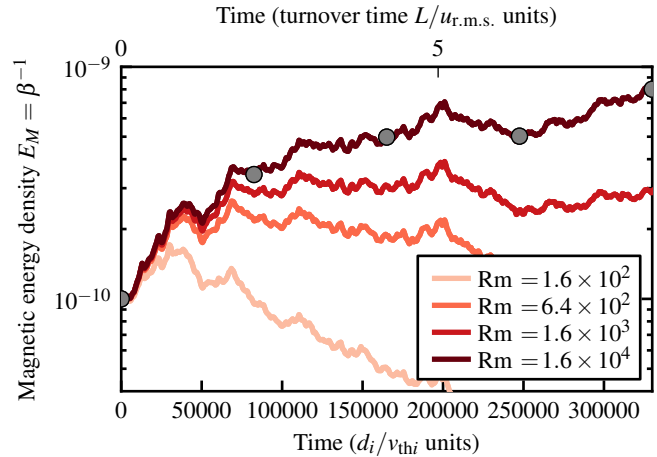


Fig. 1. Adimensionalized magnetic-energy density $E_M = \beta^{-1}$ in forced simulations with decreasing magnetic diffusivities. The flow history is identical for all simulations. $L = 2000 \pi d_i$, $k_f = 2\pi/L$, $\varepsilon = 3 \times 10^{-5} n_{i0} m_i v_{thi}^3 / d_i$, $u_{r.m.s.}/v_{thi} \approx 0.17$, and $\beta(t=0) = 10^{10}$.

Significance

While magnetic-field amplification by a dynamo effect converting kinetic flow energy into magnetic energy has long been demonstrated in conventional magnetohydrodynamic fluids, whether a similar effect is possible in more dynamically complex weakly-collisional plasmas, such as encountered in astrophysical objects on extragalactic scales, is not known. We present the first conclusive numerical evidence and dynamical picture of magnetic-field amplification by chaotic motions in a collisionless plasma. The results suggest that such a plasma dynamo may be a realizable physical effect in “laboratory-astrophysics” experiments, and support the idea that turbulent dynamos may significantly contribute to the magnetization of weakly-collisional high-energy-density astrophysical plasmas such as the intracluster medium of galaxy clusters.

Reserved for Publication Footnotes

through a turbulent collisionless plasma dynamo occurs in both unmagnetized and magnetized regimes.

Problem formulation

Our model (see Material and methods section) describes the coupled evolution of a quasi-neutral, non-relativistic plasma of collisionless protons (mass m_i), isothermal, fluid electrons of negligible inertia, and electromagnetic fields \mathbf{E} and \mathbf{B} . It formally retains magnetic advection and induction, resistivity and the Hall effect but, because of the isothermal-electrons assumption, does not allow for a Biermann battery [28] or Weibel-like instabilities [13, 29] (these effects only generate very small seed fields and are not themselves viable dynamos). The equations are solved with a 3D-3V Eulerian numerical code, in a periodic cubic spatial domain of size $L = 2000\pi d_i$, where d_i is the ion inertial length, and a velocity-space range of ± 5 ion thermal speeds v_{thi} . The system is initialized with a Maxwellian ion distribution function of uniform density n_{i0} and temperature $T_i = m_i v_{thi}^2/2$, electron temperature $T_e = T_i$, and a magnetic seed in the wavenumber range $[2\pi/L, 4\pi/L]$. The field strength, characterized by the inverse of $\beta = 8\pi n_{i0} T_i / B_{r.m.s.}^2$, remains small enough ($\beta \gg 1$) that the Hall effect is negligible, but the plasma can self-magnetize if the ion Larmor radius $\rho_i = \sqrt{\beta} d_i$ becomes smaller than L . An incompressible, non-helical, stochastic external force drives a plasma flow by injecting ion momentum at system scale ($k_f = 2\pi/L$) with a prescribed average

power density $\varepsilon = 3 \times 10^{-5} n_{i0} m_i v_{thi}^3 / d_i$. In unmagnetized regimes, the plasma is effectively very viscous due to the phase mixing of momentum by streaming ions (Landau damping), so the driving generates a smooth (forcing-scale) chaotic, subsonic, finite-amplitude flow with a correlation time $(k_f v_{thi})^{-1}$, smaller by a factor of Mach number than the turnover time $(k_f u_{r.m.s.})^{-1}$, where $u_{r.m.s.}$ is the characteristic mean ion flow velocity. This differs from fluid dynamo simulations, in which these timescales are comparable, and fast, inertial eddies de-

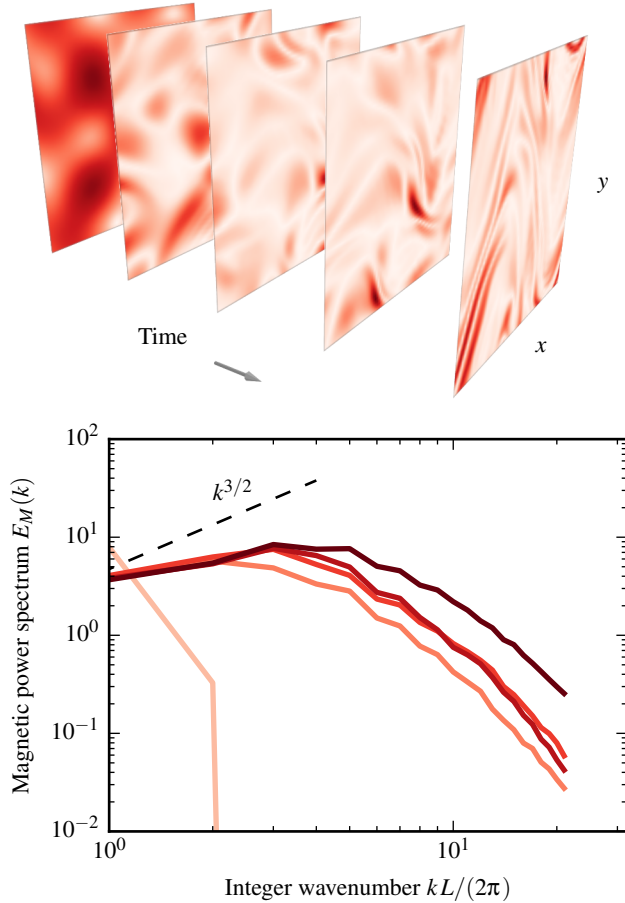


Fig. 2. Top: cross-sections of $|B|$ at increasing times (grey circles in Fig. 1) in the $Rm \approx 16000$ simulation (darker regions correspond to stronger fields, the colormap is clipped to the amplitude range of each snapshot to highlight magnetic structures). Bottom: corresponding magnetic spectra (darker lines encode increasing times).

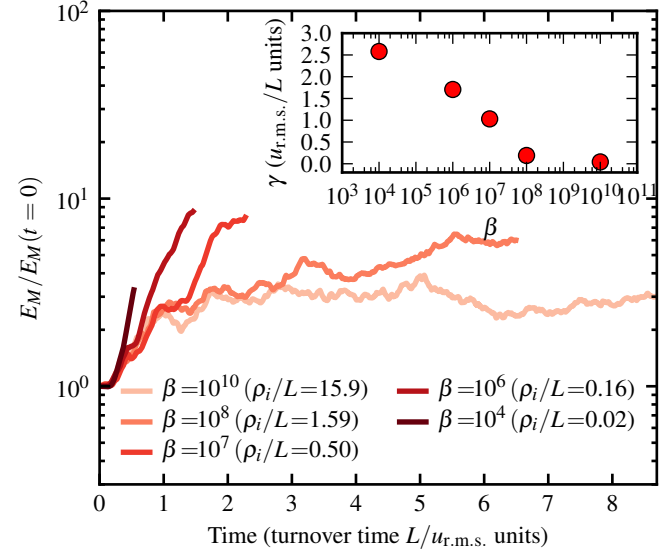


Fig. 3. Evolution of (normalized) magnetic-energy density in simulations with increasing initial magnetization (decreasing β). Inset: magnetic-energy growth rate versus β . $L = 2000\pi d_i$, $k_f = 2\pi/L$, $\varepsilon = 3 \times 10^{-5} n_{i0} m_i v_{thi}^3 / d_i$, $\eta = 0.1 d_i v_{thi}$.

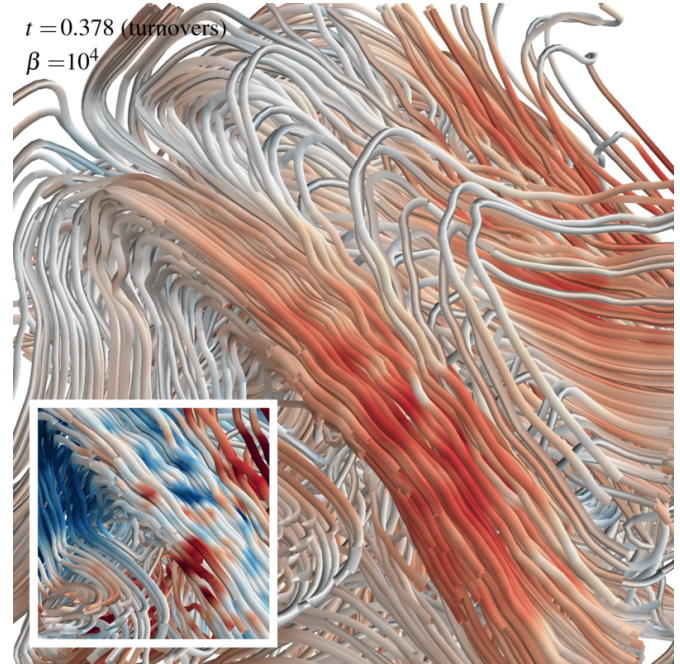


Fig. 4. Main image: 3D rendering of magnetic field lines subject to mirror and firehose instabilities in the $\beta = 10^4$ ($\rho_i/L = 0.016$) simulation (the red/blue colorscale encodes positive/negative ion pressure anisotropy Δ_i clipped to ± 1). Inset: close-up on field lines and scalar density fluctuations in the central, mirror-unstable region (the red/blue colorscale encodes $(n_i - n_{i0})/n_{i0}$ clipped to ± 1).

velop down to viscous scales. The spatial and velocity-space numerical resolution $64^3 \times 51^3$ is close to the current affordable maximum, as characterizing the dynamo requires several simulations which must be integrated for several turnover times with small timesteps to capture fast kinetic physics.

Unmagnetized regime

Figure 1 shows the evolution of magnetic energy in four unmagnetized simulations (initial $\beta = 10^{10}$, $\rho_i/L \approx 16$, $u_{r.m.s.}/v_{thi} \approx 0.17$) with magnetic diffusivities $\eta \in [0.01, 1] v_{thi} d_i$ (magnetic Reynolds numbers $Rm = u_{r.m.s.}/(k_f \eta) \in [160, 16000]$) and all other parameters fixed. The results are a conclusive demonstration of plasma dynamo, with sustained magnetic growth only occurring above a critical $Rm \approx 1600$ at this value of β . The magnetic energy growth rate is $\gamma \approx 0.16 (u_{r.m.s.}/L)$ for the largest Rm considered. Figure 2 (see also supplementary movie 1) shows two-dimensional snapshots of magnetic-field strength and the corresponding energy spectra for the growing case. The field is stretched chaotically by velocity fluctuations and develops a characteristic folded structure with reversals perpendicular to the field at the resistive scale ℓ_η [30]. The trend of the spectral evolution is consistent with the formation of a $k^{3/2}$ Kazantsev energy spectrum [1] down to $k \sim \ell_\eta^{-1}$. These results are reminiscent of a large-magnetic-Prandtl number “stretch and fold” MHD dynamo [3, 4] ($Pm = \nu/\eta$, where ν is the kinematic viscosity). Considering that the collisionless plasma flow is effectively very viscous, it is perhaps not a surprise that its dynamo action is similar to that of a random “Stokes flow” [30]. However, the critical Rm is significantly larger than in MHD. We attribute this effect to the shorter correlation time of collisionless eddies, which limits their capacity to stretch the field in a sustained fashion.

Magnetized regime

As the dynamo demonstrated above proceeds, it will take the plasma from an unmagnetized to a magnetized regime. Covering the full transition is currently computationally prohibitive, as it requires integrating the 3D-3V kinetic system over many (system-scale) fluid turnover times. We instead investigated how magnetization affects magnetic growth using several shorter simulations initialized with seed fields of identical spatial form but different strengths ($\beta \in [10^4, 10^{10}]$), using the same power input and $\eta = 0.1 v_{thi} d_i$ as in the marginally stable $Rm \approx 1600$, $\beta = 10^{10}$ case. Figure 3 shows that the magnetic-energy growth rate increases markedly with decreasing β , leading to the conclusion that magnetic growth is self-accelerating, and by implication that the critical Rm is lower at lower β (stronger seed field). We observe a transition between a “fluid-like” inductive regime, and a mixed fluid-kinetic growth regime. Figure 4 (see also supplementary movie 2) shows that ion pressure anisotropies $\Delta_i = (P_{\perp,i} - P_{\parallel,i})/P_{\perp,i}$ develop with respect to the local field in the most magnetized $\beta = 10^4$ ($\rho_i/L = 0.016$) case (\mathbf{P}_i is the ion pressure tensor, $P_{\parallel,i} = \mathbf{b}\mathbf{b} : \mathbf{P}_i$, $P_{\perp,i} = 1/2 (\text{Tr} \mathbf{P}_i - P_{\parallel,i})$, $\mathbf{b} = \mathbf{B}/|B|$). Magnetic field lines develop an angular shape in strong field-curvature regions of negative Δ_i , a nonlinear signature of the firehose instability, while bubbly mirror-like fluctuations are excited in regions of positive Δ_i where the field is stretched (small-scale magnetic depressions are associated with overdensities, see inset in Fig. 4). Relaxation of Δ_i is observed at later times in both regions. These results are consistent with theoretical expectations [12, 21, 23, 24, 27] and with a scenario in which magnetization and kinetic-scale fluctuations, by impeding the free streaming of ions, enhancing particle scattering and regulating pressure anisotropy, result in more vigorous turbulent field amplification through an effective reduction of flow viscosity [17]. Higher-resolution simulations with longer integration times than can be afforded currently are required to investigate growth in this regime quantitatively.

Discussion

This paper offers a conclusive proof-of-principle demonstration that turbulent collisionless plasma dynamo is possible. This effect involves generic plasma processes independent of any particular geometric configuration and may thus be realizable in “laboratory-astronautics” plasma experiments, provided they can achieve sufficiently weak collisionality. Numerical evidence that the dynamo becomes entangled with kinetic-scale dynamical phenomena as the plasma self-magnetizes strongly suggests that future models of weakly-collisional, magnetized turbulence in high-energy astrophysical plasmas should at least include an effective treatment of such multiscale interactions. For the time being, and while reconstructing the detailed history of cosmological magnetic fields remains out of reach observationally and computationally, our results provide a firmer physical basis for the idea that extragalactic plasma turbulence may significantly contribute to the amplification of seed cosmological fields up to dynamical levels on cosmologically short times, despite such plasmas not being simple collisional MHD fluids. The typical magnetic-field amplification timescale in the unmagnetized regime is an appreciable fraction of the eddy turnover time, and our results suggest that the dynamo self-accelerates as magnetization takes place. In the turbulent ICM where the turnover time is believed to be no longer than 10^7 years, probably much shorter [17], such a dynamo could therefore in principle bring magnetic fields from typical $10^{-21} - 10^{-9}$ (at most) Gauss seed field magnitudes [7, 8, 13, 14] to μ Gauss dynamical levels in less than a Hubble time.

New supercomputing and experimental facilities should soon make it possible to determine the parameter dependence and saturation properties of this turbulent dynamo and to further assess its relevance to the coevolutions of cosmic magnetic fields and large-scale accreting structures, which are also set to be thoroughly investigated by next-generation X-ray and radio observatories.

Materials and Methods

Hybrid kinetic system. We consider a forced, non-relativistic, quasi-neutral hybrid Vlasov-Maxwell system describing the coupled evolution of collisionless protons (mass m_i , charge e), fluid, isothermal electrons of temperature T_e and negligible inertia, and electromagnetic fields $\mathbf{E}(\mathbf{r}, t)$ and $\mathbf{B}(\mathbf{r}, t)$ (\mathbf{r} and \mathbf{v} are the spatial and velocity space coordinates). The ion distribution function $f_i(\mathbf{r}, \mathbf{v}, t)$ is governed by the Vlasov equation

$$\frac{\partial f_i}{\partial t} + \mathbf{v} \cdot \nabla f_i + \left[\frac{e}{m_i} \left(\mathbf{E} + \frac{\mathbf{v} \times \mathbf{B}}{c} \right) + \frac{\mathbf{F}}{m_i} \right] \cdot \frac{\partial f_i}{\partial \mathbf{v}} = 0,$$

where $\mathbf{F}(\mathbf{r}, t)$ is an external force described below. The ion number density is $n_i(\mathbf{r}, t) = \int f_i(\mathbf{r}, \mathbf{v}, t) d^3\mathbf{v}$, the mean “fluid” ion velocity is $\mathbf{u}_i(\mathbf{r}, t) = \int \mathbf{v} f_i(\mathbf{r}, \mathbf{v}, t) d^3\mathbf{v} / n_i$, and the ion pressure tensor is $\mathbf{P}_i(\mathbf{r}, t) = m_i \int (\mathbf{v} - \mathbf{u}_i)(\mathbf{v} - \mathbf{u}_i) f_i(\mathbf{r}, \mathbf{v}, t) d^3\mathbf{v}$. The electron number density n_e is equal to n_i at all times by quasi-neutrality. The magnetic field evolution is governed by Faraday’s equation,

$$\frac{\partial \mathbf{B}}{\partial t} = -c \nabla \times \mathbf{E},$$

and $\nabla \cdot \mathbf{B} = 0$. The electric field is calculated from Ohm’s law,

$$\mathbf{E} = -\frac{T_e \nabla n_e}{en_e} - \frac{\mathbf{u}_e \times \mathbf{B}}{c} + \frac{4\pi\eta}{c^2} \mathbf{j},$$

where $\mathbf{j} = (c/4\pi) \nabla \times \mathbf{B}$ is the current density, $\mathbf{u}_e = \mathbf{u}_i - \mathbf{j}/(en_e)$ is the mean electron velocity, and η is a uniform magnetic diffusivity. The equations are adimensionalized using the initially uniform ion density n_{i0} as a reference density, the ion inertial length $d_i = c/\omega_{pi}$, as a length scale ($\omega_{pi}^2 = 4\pi n_{i0} e^2/m_i$), and d_i/v_{thi} as a timescale. \mathbf{B} is expressed in units of $v_{thi} \sqrt{4\pi n_{i0} m_i}$, and \mathbf{E} in units of $v_{thi}^2 \sqrt{4\pi n_{i0} m_i}/c$. The adimensional magnetic energy density is the inverse of the plasma β

Numerics. The problem is solved numerically with a 3D-3V Eulerian Vlasov code [31] parallelized on 1024 cores. The resistive term in Ohm’s law is only included in Faraday’s equation to ensure that dynamo modes are numerically resolved.

Stochastic ion momentum forcing. An incompressible, non-helical, delta-correlated in time vector force $\mathbf{F}(\mathbf{r}, t)$ injecting ion momentum with a prescribed statistical power density \mathcal{E} is included in the numerical formulation of the ion Vlasov equation using a numerical technique borrowed from hydrodynamics [32]. Defining the correlation tensor of the spatial Fourier transform of the force as

$$\langle F_{\mathbf{k},i}(t) F_{\mathbf{k},j}^*(t') \rangle = \chi(k) \delta(t - t') (\delta_{ij} - k_i k_j / k^2),$$

where brackets denote ensemble averaging, it can be shown analytically that the (linear) response to this forcing in unmagnetized, collisionless regimes is a time-dependent flow $\mathbf{u}(\mathbf{r}, t)$ whose correlation tensor is

$$\langle u_{\mathbf{k},i}(t) u_{\mathbf{k},j}^*(t') \rangle = \frac{\chi(k)}{8\pi k^2} \left(\delta_{ij} - \frac{k_i k_j}{k^2} \right) \int_{-\infty}^{\infty} d\omega e^{-i\omega(t-t')} \left| Z\left(\frac{\omega}{k v_{thi}}\right) \right|^2,$$

where $Z(\zeta)$ is the plasma dispersion function [33]. For the forcing parameters considered here, we checked that the correlation tensor of the actual subsonic, chaotic flow driven at $k = k_f$ in unmagnetized simulations is of this form to a very good approximation, with an effective correlation time $(k_f v_{thi})^{-1}$.

Appendix: Movies

1. Kazantsev, AP (1968) Enhancement of a magnetic field by a conducting fluid. Soviet Phys JETP 26:1031.
2. Moffatt, HK (1977) Magnetic Field Generation In Electrically Conducting fluids. Cambridge University Press.
3. Zel'dovich, YB, Ruzmaikin, AA, Molchanov, SA, Sokoloff, DA (1984) Kinematic dynamo problem in a linear velocity field. J Fluid Mech 144:1.
4. Childress, S & Gilbert, AD (1995) Stretch, Twist, Fold. The Fast Dynamo. Springer-Verlag.
5. Meneguzzi M, Frisch, U & Pouquet, A (1981) Helical and nonhelical turbulent dynamos. Phys Rev Lett 47:1060.
6. Monchaux, R et al. Generation of a magnetic field by dynamo action in a turbulent flow of liquid sodium. Phys Rev Lett 98, 044502 (2007).
7. Kulsrud, RM & Zweibel, EG (2008) On the origin of cosmic magnetic fields. Rep Prog Phys 71:046901.
8. Durrer, D & Neronov, A (2013) Cosmological magnetic fields: their generation, evolution and observation. Astron. & Astrophys Rev 21:62.
9. Zweibel, EG & Heiles, C (1997) Magnetic fields in galaxies and beyond. Nature 385:131.
10. Carilli, CL & Taylor, GB (2002) Cluster magnetic fields. Annu Rev Astron Astr 40:319.
11. Vogt, C & Enßlin, TA (2005) A Bayesian view on Faraday rotation maps – Seeing the magnetic power spectra in galaxy clusters. Astron Astrophys 434:67.
12. Schekochihin, AA, Cowley, SC, Kulsrud, RM, Hammett, GW & Sharma, P (2005) Plasma instabilities and magnetic field growth in clusters of galaxies. Astrophys J 629:139.
13. Medvedev, MV, Silva, LO & Kamionkowski, M (2006) Cluster magnetic fields from large-scale structure and galaxy cluster shocks. Astrophys J Lett 642:L1.
14. Ryu, D, Kang, H, Cho, J & Das, S (2008) Turbulence and magnetic fields in the large-scale structure of the universe. Science 320:909.
15. Vazza, F, Brüggemann, M, Gheller, C & Wang, P (2014) On the amplification of magnetic fields in cosmic filaments and galaxy clusters. Mon Not R Astron Soc 445:3706.
16. Santos-Lima, R et al. (2014) Magnetic field amplification and evolution in turbulent collisionless magnetohydrodynamics: an application to the intracluster medium. Astrophys J 781:84.
17. Mogavero, F & Schekochihin, AA (2014) Models of magnetic field evolution and effective viscosity in weakly collisional extragalactic plasmas. Mon Not R Astron Soc 440:3226.
18. Miniati, F and Beresnyak, A (2015) Self-similar energetics in large clusters of galaxies. Nature 523:59.

ACKNOWLEDGMENTS. The authors thank S. C. Cowley and M. W. Kunz for many valuable discussions and suggestions, and C. Cavazzoni (CINECA, Italy) for his essential contribution to the code parallelisation and performance. This work was granted access to the HPC resources of IDRIS under the allocation 2015-i2015047188 made by GENCI, and of CINECA under ISCRA-B allocation COLDYN.

Fig. 5. Movie 1: (http://userpages.irap.omp.eu/~frincon/vlasov_dynamo/movie1.mp4): Three-dimensional animated rendering of the dynamical evolution of magnetic field lines and magnetic-field strength in the unmagnetized $\beta = 10^{10}$ dynamo simulation of Fig. 2 (darker red regions correspond to stronger fields. Unlike in Fig. 2, the same colorscale is used at all times to highlight the overall growth of magnetic energy and its localization).

Fig. 6. Movie 2: (http://userpages.irap.omp.eu/~frincon/vlasov_dynamo/movie2.mp4): Three-dimensional animated rendering of the dynamical evolution of magnetic field lines and local ion pressure anisotropy Δ_i in the magnetized $\beta = 10^4$ ($\rho_i/L = 0.016$) simulation. Magnetic field lines develop an angular shape in strong field-curvature regions of negative Δ_i (blue), a nonlinear signature of the firehose instability, while bubbly mirror-like fluctuations are excited in regions of positive Δ_i (red) where the field is stretched.

19. Forest, CB et al. (2015) The Wisconsin Plasma Astrophysics Laboratory. J Plasma Phys 81:345810501.
20. Meinecke, J et al. (2015) Developed turbulence and nonlinear amplification of magnetic fields in laboratory and astrophysical plasmas. Proc Natl Acad Sci USA 112:8211.
21. Schekochihin, AA, Cowley, SC, Kulsrud, RM, Rosin, MS & Heinemann, TH (2008) Nonlinear growth of firehose and mirror fluctuations in astrophysical plasmas. Phys Rev Lett 100:081301.
22. Schaeffer, K, Drake, JF & Swisdak, M (2011) The effects of plasma beta and anisotropy instabilities on the dynamics of reconnecting magnetic fields in the heliosheath. Astrophys J 743:70.
23. Kunz, MW, Schekochihin, AA & Stone, JM (2014) Firehose and mirror instabilities in a collisionless shearing plasma. Phys Rev Lett 112:205003.
24. Riquelme, MA, Quataert, E & Verscharen, D (2015) Particle-in-cell simulations of continuously driven mirror and ion cyclotron instabilities in high beta astrophysical and heliospheric plasmas. Astrophys J 800:27.
25. Sironi, L & Narayan, R (2015) Electron Heating by the Ion Cyclotron Instability in Collisionless Accretion Flows. I. Compression-driven Instabilities and the Electron Heating Mechanism. Astrophys J 800:88.
26. Hellinger, P & Trávníček, PM (2015) Proton temperature-anisotropy-driven instabilities in weakly collisional plasmas: Hybrid simulations. J Plasma Phys 81:305810103.
27. Rincon, F, Schekochihin, AA & Cowley, SC (2015) Non-linear mirror instability. Mon Not R Astron Soc 447:L45.
28. Biermann, L (1950) Über den ursprung der magnetfelder auf sternern und im interstellaren raum. Z Naturf 5:65.
29. Weibel, ES (1959) Spontaneously growing transverse waves in a plasma due to an anisotropic velocity distribution. Phys Rev Lett 2:83.
30. Schekochihin, AA, Cowley, SC & Taylor SF (2004) Simulations of the small-scale turbulent dynamo. Astrophys J 612:276.
31. Valentini, F, Trávníček, P, Califano, F, Hellinger, P & Mangeney, A (2007) A hybrid-Vlasov model based on the current advance method for the simulation of collisionless magnetized plasma. J Comp Phys 225:753.
32. Alvelius, K (1999) Random forcing of three-dimensional homogeneous turbulence. Phys Fluids 11:1880.
33. Fried, BD & Conte, SD (1961) The Plasma Dispersion Function. New York: Academic Press.